INTERNATIONAL ATOMIC ENERGY AGENCY
UNITED NATIONS EDUCATIONAL, SCIENTIFIC AND CULTURAL ORGANIZATION
INTERNATIONAL CENTRE FOR THEORETICAL PHYSICS
I.C.T.P., P.O. BOX 586, 34100 TRIESTE, ITALY. CABLE: CENTRATOM TRIESTE

SMR.380/15

COLLEGE ON THEORETICAL AND EXPERIMENTAL RADIOPROPAGATION SCIENCE

6 - 24 February 1989

LECTURES 3&4: PRECIPITATION AND ATMOSPHERIC GASES

G.O. AJAYI

Department of Electronic and Electrical Engineering
Obafemi Awolowo University
Ile-Ife, Nigeria

TABLE OF CONTENTS

1. INTRODUCTION

The congestion in the low microwave frequency bands and the increasing need for high capacity communication channels have necessitated the use of frequencies above 10 GHz for both terrestrial and satellite communication systems. Hydrometeors such as rain, hail, fog, ice, cloud and snow attenuate radio waves above 5 GHz and also cause other impairments to communication systems. The most important effects of hydrometeors on microwave propagation are (Ippolito, 1981):

(a) Attenuation caused by dissipation of radio wave energy as heat.

(b) Scatter resulting in loss in the desired direction and consequently causing interference to other systems. Scatter loss can dominate when the wavelength is much smaller than hydrometer size.

(c) Depolarization due to the non-spherical nature of rain drops.

(d) Rapid amplitude and phase scintillations caused by equivalent multipath propagation.

(e) Antenna gain degradation due to phase dispersion of ray paths reaching the antenna.

(f) Bandwidth coherence reduction especially in digital systems involving carriers spanning over large channel bandwidths.

The effect of rain is the most serious of all the hydrometeors. Attenuation and depolarization due to rain will be mostly considered.

1.1 TYPES of RAIN

Stratiform Rain – widespread regions with low rain rates and small embedded showers, with horizontal extent of hundreds of km and durations exceeding one hour. The rain vertical extent is up to the height of the bright band.

Convective Rain – Localized areas of relatively intense rainfall characterized by strong up- and down-drafts extending deep into the troposphere. The horizontal scale is of several km and durations of tens of minutes.

Orographic – caused entirely or mostly by the forced uplift of moist air over high ground.

Monsoon Rain – A sequence of bands of intense convection followed by intervals of stratiform rain. The bands are typically 50 km across, hundreds of km in length and produce heavy precipitation lasting for several hours.

Tropical Storms – Large regions of precipitation extending over hundreds of km. The storms are characterized by several spiral bands terminating in regions of intense precipitation surrounding the central region of the storm.

2 Drop size Distribution

The three most commonly used distributions obtained mainly from temperate data are

Laws and Parsons LP
Marshall – Palmer MP
Joss – thunderstorm J-T and drizzle (J-D)

The measurements of Laws and Parsons (1943) and Marshall and Palmer (1948) are fitted by a negative exponential of the form

$$N_D = N_0 e^{-\Lambda D} \quad \text{---(1)}$$

where $\Lambda = A R^{-0.21}$ ---(2)

and $N(D)$ = number of drops per mm diameter interval per cubic metre
$N_0 = 8000\ m^{-3} mm^{-1}$ and
$A = 4.1$

Joss et al employed three classifications for rain events with different constants for the general exponential distribution given in Table 1 below

Type of rain	N_0	A
Drizzle	30,000	5.7
Widespread rain	8,000	4.1
Thunderstorm	1,400	3.0

Table 1 Joss et al classification of rainfall

The M-P distribution satisfies the rain rate equation making use of the fall velocity of the raindrops, but this is not true of

the distributions of Joss et al. for example for R of 100 mm h^{-1} used in the thunderstorm distribution, the true rain rate calculated from the volume of water falling is only 67 mm h^{-1}

2.1 Tropical raindrop size distribution

Making use of the raindrop size distribution measured in Nigeria, Ajayi and Olsen,[83] showed that the modified gamma distribution gave a better fit than the M-P or L-P distribution. The modified gamma distribution is given by

$$N(D) = 0.070\, D^{1.43} \exp\left(-386\, R^{-0.432} D^{2.6}\right)$$

for $R \leq 15$ mm h^{-1} — — (3)

and

$$N(D) = 0.056\, D^{1.43} \exp\left(-895\, R^{-0.515} D^{3.1}\right)$$

for $R > 15$ mm h^{-1} — — (4)

It was later shown that tropical data could well be fitted with a log-normal distribution. Ajayi-Olsen, 1985 proposed the following tropical model.

$$N(D) = \frac{N_T}{\sigma D \sqrt{2\pi}} \exp\left\{-\frac{1}{2}\left(\frac{\ln D - \mu}{\sigma}\right)^2\right\} \quad — — (5)$$

where μ is the mean of $\ln D$, σ is the standard deviation, and N_T is the total number of drops of all sizes.

$$N_T = 108\, R^{0.363} \quad — — 6(a)$$

$$\mu = -0.195 + 0.199 \ln R \quad — — 6(b)$$

$$\sigma^2 = 0.137 - 0.013 \ln R \quad — — 6(c)$$

Fig. 1 shows the comparison between M-P, modified

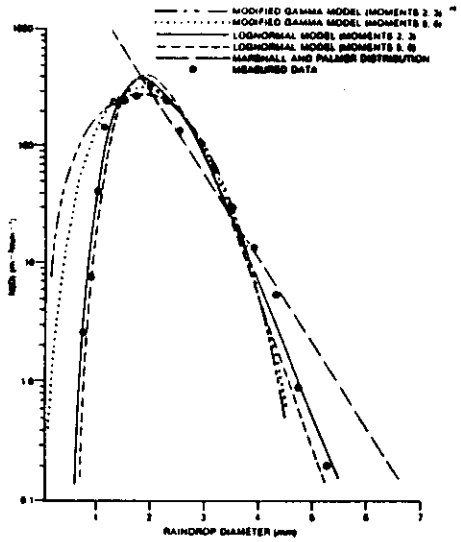

Fig. 1 Comparison of measured, modified gamma, lognormal and Marshall-Palmer distributions at 75 mm h^{-1}. Circles, measured data; long and short dashes, modified gamma model (moments 2, 3); dotted line, modified gamma model (moments 5, 6); solid line, lognormal model (moments 2, 3); short dashes, lognormal model (moments 5, 6); long dashes, Marshall-Palmer distribution. [Ajayi and Olsen, 1985]

gamma distribution, and the Ajayi-Olsen (A-O) lognormal distribution. The M-P overestimates both the small and the large diameter drop number for the tropical region.

3 SHAPE OF RAINDROPS

For simplified calculations, spherical drops are assumed. However, falling drops assume a nearly spheroidal shape when subject only to the effects of gravity and the surface tension of water. The force of gravity provides the major orientation force for raindrops. The drops may vibrate and oscillate while falling, but the net shape is oblate spheroidal with the symmetry axis close to vertical. Pruppacher and Pitter (1971) proposed a shape that is a function of drop size.

4 RAINFALL RATE DISTRIBUTION

A model for the rain rate distribution is given by CCIR as

$$P(R \geq r) = \frac{a e^{-ur}}{r^b} \qquad r \geq 2 \text{ mm/h} \quad \text{--- (7)}$$

where a and b are derived from the rain rate $R_{0.01}$ exceeded 0.01% of the time (Manfouma, 1985 a) and u is the parameter depending on climate and geographical features.

$$a = 10^{-4} R_{0.01}^{b} \exp(u R_{0.01}) \quad \text{--- (8)}$$

$$b = 8.22 R_{0.01}^{-0.584} \quad \text{--- (9)}$$

and the values of u given in Table 2 (Manfouma, 1985 b, 1987) provide a good fit to the distributions observed at most locations.

Localities	Temperate zones					Tropical zones
	EUROPE		AMERICA		JAPAN	
	Central Southern	Northern	Canada	USA		
- Coastal or nearby water masses and mountainous regions	0.030	0.045	0.032	0.032	0.045	0.042
- Average rolling terrain	0.025	0.025	0.025	0.025	0.045	0.025
- Arid regions			0.015	0.015		

Table 2: Classification of parameter u values

Fig. 2 shows CCIR rain climatic zones with values given in Table 3. Fig. 3 also shows the CCIR rainfall contours for rate exceeded for 0.01% of time. Fig. 4 (a) (Manfouma, 1987) shows some cumulative rain rate distributions in tropical zone, while figure 4 (b) (Ajayi and Olsha, 1984) shows the cumulative rainfall distributions for various integration times for a location in Nigeria.

5 RAIN ATTENUATION

Rain drops both absorb and scatter microwave energy. Both may contribute to the attenuation on a radio path, while scatter may also cause interference between radio paths. At wavelengths long compared with the drop size, attenuation due to absorption will be greater than that due to scatter, while at the shorter wavelengths, scatter will predominate. The Rayleigh scattering theory appears to apply only up to 3 GHz (Ippolito et al. 1981) while above 3 GHz, Mie scattering is the primary technique for rain attenuation calculations.

The specific attenuation γ (dB/km) due to rain

Fig. 2 : Rain climatic zones (Refer to Table 3)

[CCIR, 1988]

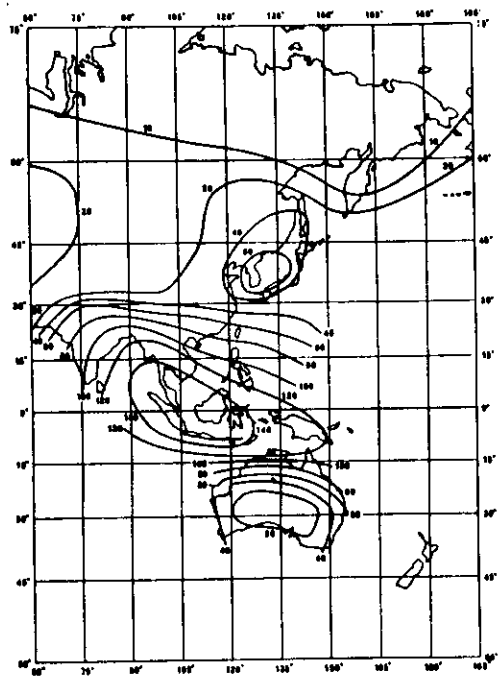

Figure 3

[CCIR, 1988]

TABLE 3 - *Rain climatic zones* [CCIR, 1982].

Rainfall intensity exceeded (mm/h) (Reference to Fig 2

Percentage of time (%)	A	B	C	D	E	F	G	H	J	K	L	M	N	P
1.0	-	1	-	3	1	2	-	-	-	2	-	4	5	12
0.3	1	2	3	5	3	4	7	4	13	6	7	11	15	34
0.1	2	3	5	8	6	8	12	10	20	12	15	22	35	65
0.03	5	6	9	13	12	15	20	18	28	23	33	40	65	105
0.01	8	12	15	19	22	28	30	32	35	42	60	63	95	145
0.003	14	21	26	29	41	54	45	55	45	70	105	95	140	200
0.001	22	32	42	42	70	78	65	83	55	100	150	120	180	250

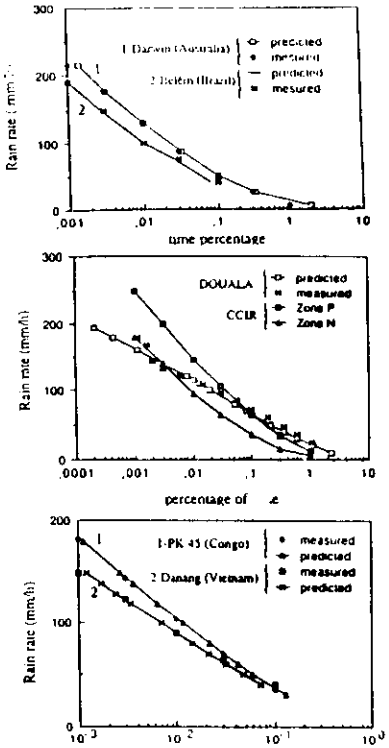

Fig. 4(a) Cumulative rain distribution in tropical zones. (After Moupfouma, 1987).

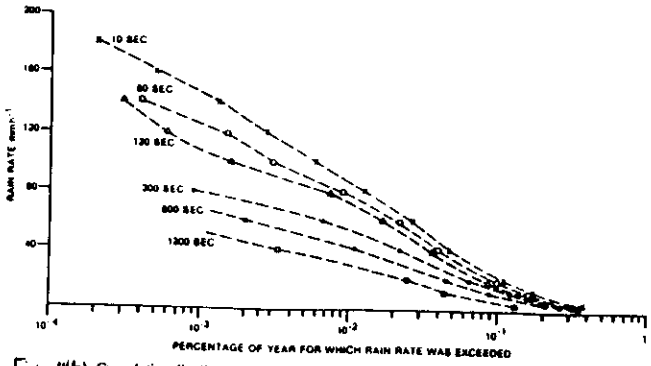

Fig. 4(b) Cumulative distributions of rain rate at Ile-Ife for different gage integration times. Average for September 1979–December 1981.

$$Q_t(D) = Q_s(D) + Q_A(D) \quad \text{---(11)}$$

where Q_s and Q_A are scattering and absorption cross sections respectively.

$Q_t(D)$ is a function of drop size diameter, wavelength and complex refractive index m of the water drop.

$N(D)$ is number of drops per unit volume per diameter interval.

The rain rate is related to the drop size distribution by

$$R = 6\pi \times 10^{-4} \int_0^\infty D^3 N(D) V(D) dD \quad \text{---(12)}$$

where $V(D)$ = terminal velocity of drops in $m s^{-1}$ and $N(D)$ is in $mm^{-1} m^{-3}$

The specific attenuation has been found to be related to rainfall rate, R as

$$\gamma = a(f) R^{b(f)} \quad \text{---(13)}$$

where $a(f)$ and $b(f)$ are dependent on the frequency, polarization and the raindrop characteristics.

Table 4 shows the values of a and b CCIR, 1982 assuming Laws and Parson's rain drop size distribution

The analytical approximations for $a(f)$ and $b(f)$, adequate for system engineers are given by (Olsen et al. 1978)

TABLE 4 *Regression coefficients for estimating specific attenuations* (CCIR, 1982)

Frequency (GHz)	a_H	a_v	b_H	b_v
1	0.0000387	0.0000352	0.912	0.880
2	0.000154	0.000138	0.963	0.923
4	0.000650	0.000591	1.121	1.075
6	0.00175	0.00155	1.308	1.265
7	0.00301	0.00265	1.332	1.312
8	0.00454	0.00395	1.327	1.310
10	0.0101	0.00887	1.276	1.264
12	0.0188	0.0168	1.217	1.200
15	0.0367	0.0335	1.154	1.128
20	0.0751	0.0691	1.099	1.065
25	0.124	0.113	1.061	1.030
30	0.187	0.167	1.021	1.000
35	0.263	0.233	0.979	0.963
40	0.350	0.310	0.939	0.929
45	0.442	0.393	0.903	0.897
50	0.536	0.479	0.873	0.868
60	0.707	0.642	0.826	0.824
70	0.851	0.784	0.793	0.793
80	0.975	0.906	0.769	0.769
90	1.06	0.999	0.753	0.754
100	1.12	1.06	0.743	0.744
120	1.18	1.13	0.731	0.732
150	1.31	1.27	0.710	0.711
200	1.45	1.42	0.689	0.690
300	1.36	1.35	0.688	0.689
400	1.32	1.31	0.683	0.684

*Raindrop size distribution [Laws and Parsons, 1943].
Terminal velocity of raindrops [Gunn and Kinzer, 1949].
Index of refraction of water at 20°C [Ray, 1972].

Table 5: Comparison of a and b in the Relation aR^b for Specific Attenuation (Ajayi, 1985).

Freq (GHz)	a				b			
	HP		VP		HP		VP	
	AJAYI	CCIR	AJAYI	CCIR	AJAYI	CCIR	AJAYI	CCIR
1	.352(-4)*	.3887(-4)	.3100(-4)	.3516(-4)	.9273	.9116	.9040	.8802
2	.1421(-3)	.1538(-3)	.1240(-3)	.1384(-3)	.9627	.9633	.9333	.9234
4	.651(-3)	.6409(-3)	.5732(-3)	.5910(-3)	1.073	1.131	1.043	1.075
6	.188(-2)	.1745(-2)	.1636(-2)	.1547(-2)	1.214	1.307	1.177	1.265
8	.472(-2)	.4536(-2)	.4102(-2)	.3948(-2)	1.273	1.327	1.283	1.310
10	.106(-1)	.1010(-1)	.9238(-2)	.8870(-2)	1.252	1.276	1.242	1.264
12	.203(-1)	.1882(-1)	.1774(-1)	.1681(-1)	1.204	1.217	1.199	1.200
15	.401(-1)	.3688(-1)	.3509(-1)	.3347(-1)	1.139	1.154	1.136	1.128
20	.819(-1)	.7500(-1)	.7477(-1)	.6908(-1)	1.083	1.099	1.057	1.065
25	.1335	.1244	.1208	.1130	1.055	1.061	1.026	1.030
30	.198	.1871	.1781	.1674	1.024	1.020	[illegible]	.9997
35	.276	.2620	.2478	.2334	.8868	.9788	.9687	.9833
40	.367	.3485	.3328	.3098	.9437	.9381	.9338	.9287
45	.466	.4424	.4097	.3932	.9023	.8832	.8963	.8960
50	.582	.5368	.4984	.4793	.8649	.8728	.8617	.8863
55	.681	.6251	.5833	.5632	.8336	.8471	.8321	.8443
60	.727	.7089	.6568	.6418	.8089	.8281	.8078	.8243
65	.781	.7816	.7213	.7148	.7885	.8083	.7880	.8073
70	.8474	.8514	.7779	.7838	.7713	.7930	.7713	.7928
75	.897	.9167	.8281	.8477	.7563	.7788	.7578	.7799
80	.939	.9763	.8714	.8983	.7441	.7687	.7453	.7803
85	.972	1.025	.9064	.9572	.7340	.7588	.7388	.7606
90	.994	1.064	.9321	.9902	.7279	.7529	.7393	.7537
95	1.007	1.084	.9490	1.033	.7238	.7478	.7248	.7483
100	1.011	1.116	.9490	1.059	.7209	.7434	.7221	.7461
120	.988	1.177	.9517	1.132	.7209	.7313	.7215	.7320
150	.968	1.310	.9367	1.287	.7168	.7005	.7187	.7112
200	.954	1.448	.9382	1.420	.7092	.6887	.7104	.6899
300	.905	1.384	.9082	1.349	.7096	.6878	.7110	.6890
400	.862	1.318	.8584	1.308	.7060	.6837	.7060	.6841

CCIR: assumes Laws and Parsons drop size model

Ajayi: current study assuming Ajayi-Olsen (1985) tropical drop size model.

*(-4) is an abbreviation for 10^{-4}, and so on

HP and VP indicate horizontal and vertical polarizations respectively

$$a(f) = 4.21 \times 10^{-5} (f)^{2.42} \qquad 2.9 \le f \le 54\ \text{GHz}$$

$$= 4.09 \times 10^{-2} (f)^{0.699} \qquad 54 \le f \le 180\ \text{GHz} \qquad \text{---} \ 14(a)$$

and

$$b(f) = 1.41 (f)^{-0.0779} \qquad 8.5 \le f \le 25\ \text{GHz}$$

$$= 2.63 (f)^{-0.272} \qquad 25 \le f \le 164\ \text{GHz} \qquad \text{---} \ 14(b)$$

where f is in GHz

Table 5 gives the values of a and b obtained from Ajayi - Olsen rain drop size distribution, which is considered more adequate for tropical regions. The values are compared with those of CCIR. Figure 5 gives the specific attenuation as a function of frequency and rain rate. Figure 6 compares the CCIR specific attenuation with those computed using Ajayi and Olsen models for oblate spheroidal drops.

5.1 Frequency Scaling

When reliable long-term attenuation statistics are available at one frequency f, the attenuation at another frequency f_2 can be estimated in the range 7 to 50 GHz, for the same hop length and in the same climatic region.

$$\frac{A_1}{A_2} = \frac{g(f_1)}{g(f_2)} \qquad \text{---} \ (15)$$

where A_1 and A_2 are the values of attenuation in dB at frequencies f_1 and f_2 (in GHz) exceeded with equal probability and (CCIR, 1988) gives

$$a(f) = f^{1.72} \qquad \text{---} \ (16)$$

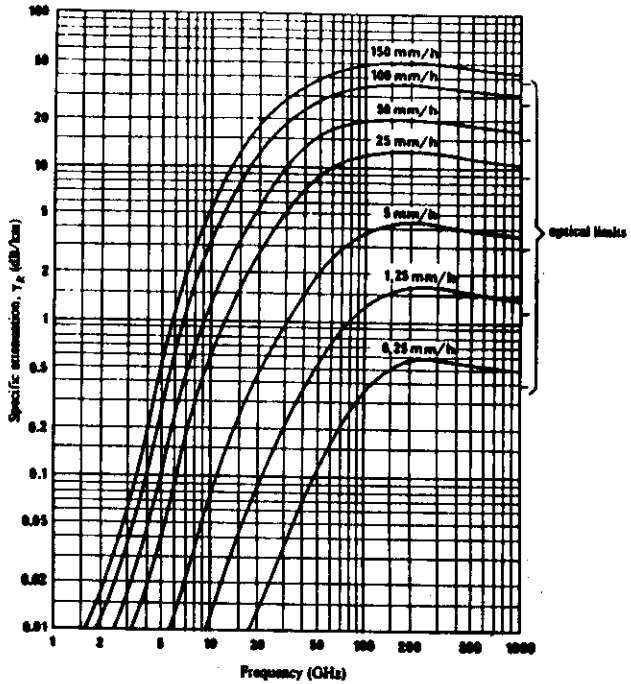

FIGURE 5 - *Specific attenuation γ_R due to rain* [CCIR, 1982]

Raindrop size distribution [Laws and Parsons, 1943]
Terminal velocity of raindrops [Gunn and Kinzer, 1949]
Index of refraction of water at 20° C [Ray, 1972]
Spherical drops

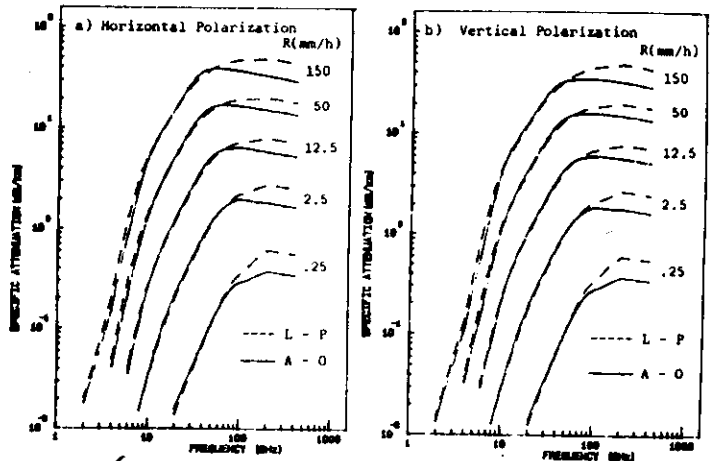

Figure 6 Specific Attenuation using Ajayi-Olsen (A - O) and Laws and Parsons (L - P) raindrop size distributions. Temperature of 20°c.

6 Rain induced depolarization

In "frequency reuse systems" employing orthogonal polarization, the interfering crosstalk between the two channels through depolarization caused by raindrops can severely restrict the utility of such a system. The degree of depolarization may be represented by the ratio of cross polarized to copolarized signals at the receiver. Depolarization by hydrometeors is considered to be due to the non-sphericity of the hydrometeors and in addition, for linear polarizations, due to the difference between polarization angle and mean orientation angle of the hydrometeors. Depolarization has became an important topic because terrestrial and earth-space microwave communication links could use two orthogonal polarizations at the same frequency to increase channel capacity and depolarization will limit the use of these two communication channels.

The cross polarization discriminations are given by

$$XPD_H = 20 \log |\Delta E_V / E_H| \quad --- (17)$$

$$XPD_V = 20 \log |\Delta E_H / E_V| \quad --- (18)$$

where ΔE_H = cross-polarized received field in the direction E_H transferred from E_V, and ΔE_V is the cross-polarized received field in the direction E_V transferred from E_H. H and V refer to horizontal and vertical polarizations respectively.

The XPD is dependent on the differential attenuation and differential phase shift. The rain induced attenuation and phase-shift can also be expressed as [Maggori, 1981).

$$\alpha = 4.343 \times 10^3 \frac{\lambda^2}{\pi} \sum Re[S_{H,V}] N(D) \Delta D \quad dB/km \quad --- (19)$$

$$\phi = 90 \times 10^3 \left(\frac{\lambda}{\pi}\right)^2 \sum Im[S_{H,V}] N(D) \Delta D \quad deg/km \quad --- (20)$$

where $S_{H,V}$ is the forward scattering amplitude function, λ is in metre, $N(D)\Delta D$ in number per cubic metre.

The XPD is given by Oguchi, 1983 as

$$XPD_H = 20 \log \left| \frac{(1-G)\tan\theta}{G + \tan^2\theta} \right| \quad --- (21)$$

$$XPD_V = 20 \log \left| \frac{(1-G)\tan\theta}{1 + G\tan^2\theta} \right| \quad --- (22)$$

where θ = canting angle of raindrops and G is given by

$$G = \exp[-(\Delta\alpha + j\Delta\phi)L] \quad --- (23)$$

where $\Delta\alpha$ = differential attenuation in nepers per unit length and $\Delta\phi$ is differential phase shift in degrees per unit length. Gaussian canting angle distribution can be assumed.

In terms of co-polarized path attenuation (CPA), we have (CCIR),

$$XPD = U - V \log(CPA) \quad dB \quad --- (24)$$

where $U = C(f) + D(\varepsilon) + K^2 + I(\tau) \quad --- 25(a)$

U and V depend primarily on f (GHz), path elevation angle ε and polarization tilt angle τ (for linear polarization) relative to the horizontal. C(f) and V(f) also depend — to some extent on drop size distribution, drop shape distribution and drop temperature.

$$C(f) = 30 \log(f) \qquad 8 \le f \le 35\,\text{GHz} \qquad -(26)$$

assuming Pruppacher–Pitter drop-shape, Laws and Parsons drop size distribution at a temperature of 20°C (CCIR).

$$D(\varepsilon) = -40 \log(\cos \varepsilon) \qquad - - - (27)$$

for a Gaussian model of raindrop canting angle distribution

$$\kappa^2 = 0.0053\, \sigma^2 \qquad - - - (28)$$

where σ (degrees) is the effective standard deviation of the raindrop canting angle distribution.

$$J(\tau) = -10 \log \tfrac{1}{2}\left[1 - \cos(4\tau) \exp(-\kappa_m^2)\right] \; - - -(29)$$

$$\text{where } \kappa_m^2 = 0.0024\, \sigma_m^2 \qquad - - - (30)$$

σ_m (degrees) is the standard deviation of a zero mean Gaussian distribution of the effective raindrop canting angle φ.

Figures 7, 8, 9 show the variation of differential attenuation, phase shift and XPD for spheroidal and Pruppacher–Pitter drop shapes.

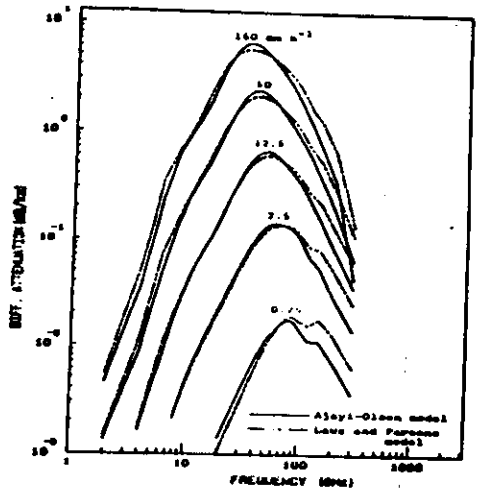

[After Ajayi et al., 1987]

Fig. 7 : Differential attenuation for oblate spheroidal drops using the Ajayi-Oleon and the Laws and Parsons dropsize distributions with the FSA Mugaturi at 20°C.

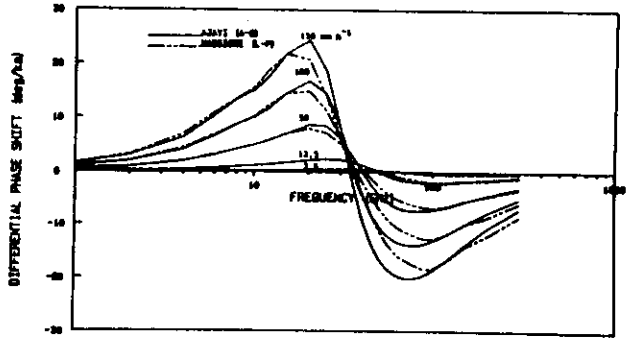

Figure 8 : Effect of dropsize distribution on differential phase shift using the Ajayi - Oleen (A-O) and the Laws and Parsons (L-P) dropsize distributions.

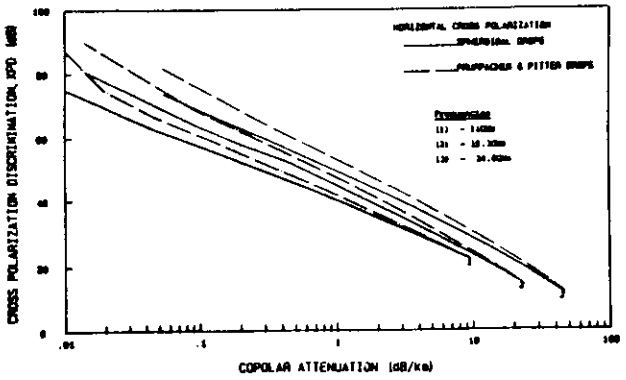

Figure 9 : Variation of cross polarization discrimination, XPD with copolar attenuation CPA at three frequencies showing the effect of rain drop shape.

7 Attenuation by Atmospheric Gases

Molecular absorption at centimetre and mm wavelengths is primarily due to atmospheric water vapour and oxygen. The oxygen molecule has a small magnetic moment and absorption is produced by magnetic interaction with the incident field. The interaction produces a series of very close lines between about 50 and 70 GHz and an isolated line at 119 GHz (Crane, 1981). Oxygen does not change with latitude or season, but diurnal and seasonal variations of water vapour can be extremely large. The electric dipole associated with the water vapour molecule interacts with the electromagnetic radiation to produce rotation absorption lines at 22.2, 183.3 and 324 GHz. The thermal emission at frequencies near the peaks of the water vapour lines is also proportional to the number of water vapour molecules and may be used to sense the water vapour concentration when the temperature is known. (Reddy, 1987).

The total gaseous absorption in the atmosphere, A_a(dB) over a path length r_0 (km) is given by

$$A_a = \int_0^{r_0} \gamma_a(r)\, dr \qquad \text{---(31)}$$

where $\gamma_a(r) = \gamma_o(r) + \gamma_w(r)$ ---(32)

$\gamma_a(r)$ is the specific attenuation (dB km^{-1}) and $\gamma_o(r)$ and $\gamma_w(r)$ are the contributions by oxygen and water vapour respectively.

For dry air, the specific attenuation at ground level (pressure = 1013 mb) and at a temperature of 15°C is mainly due to oxygen and is given by (Gibbins, 1986).

$$\gamma_o = \left[7.19\times10^{-3} + \frac{6.09}{f^2+0.227} + \frac{4.81}{(f-57)^2+1.50}\right] f^2 \times 10^{-3} \quad \text{dB/km}$$

for $f < 57$ GHz ---(33)

$$\gamma_o = \left[3.79\times10^{-7} f + \frac{0.265}{(f-63)^2+1.59} + \frac{0.028}{(f-118)^2+1.47}\right] (f+198)^2 \times 10^{-3} \quad \text{dB/km}$$

for $f > 63$ GHz ---(34)

where f is the frequency (GHz).

For water vapour, the specific attenuation at sea level, at a temperature of 15°C, and including the effects of the quadratic dependence on water vapour density, is given by (Gibbins, 1986)

$$\gamma_w = \left\{0.050 + 0.0021\rho + \frac{3.6}{(f-22.2)^2+8.5} + \frac{10.6}{(f-183.3)^2+9.0} + \frac{8.9}{(f-325.4)^2+26.3}\right\} f^2 \rho\, 10^{-4} \quad \text{dB/km}$$

for $f < 350$ GHz ---(35)

f is frequency in GHz and ρ is the water vapour density in g/m^3.

figure 10 (CCIR, 1982) shows attenuation due to gaseous constituents and precipitation for transmission through the atmosphere. Fig. 11 shows the gaseous specific attenuation, whilst fig. 12 compares the CCIR and the values of specific attenuation obtained in Nigeria.

7.1 Path Attenuation

For terrestrial paths, the path attenuation is given by

$$A_a = \gamma_a r_0 = (\gamma_0 + \gamma_w) r_0 \quad - - - (35)$$

where r_0 = path length

For slant paths, total attenuation is obtained by integrating equation (1) through the atmosphere

7.1.1 Frequencies outside the range 57-63 GHz.

The equivalent height concept is based on the assumption of an exponential atmosphere specified by a scale height to describe the decay in density with altitude. The equivalent heights are given by (CCIR, 1988)

$$h_0 = 6 \text{ km} \qquad f < 57 \text{ GHz} \quad - (36)$$

$$h_0 = 6 + \frac{4.0}{(f-118.7)^2 + 1} \text{ km} \qquad 63 < f < 350 \text{ GHz} \quad - (37)$$

$$h_w = h_{w0}\left\{1 + \frac{3.0}{(f-22.2)^2+5} + \frac{5.0}{(f-183.3)^2+6} + \frac{2.5}{(f-325.4)^2+4}\right\} \text{ km}$$

for $f < 350$ GHz $\quad - (38)$

Outside the absorption bands, $h_0 \approx 6$ km and $h_w \approx 2$ km depending on weather conditions

$$A_a = \gamma_0 h_0 + \gamma_w h_w \quad - \quad - \quad (39)$$

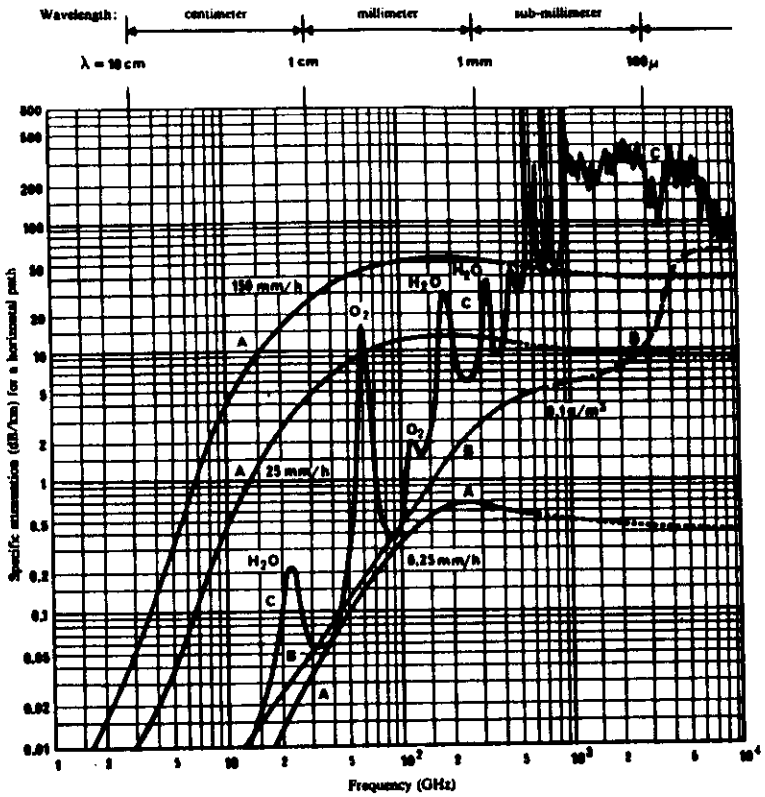

FIGURE 10– *Attenuation due to gaseous constituents and precipitation for transmissions through the atmosphere*

Temperature: 20° C
Pressure: sea level: 1 atm
Water vapour: 7.5 g/m³

A: rain
B: fog
C: gaseous

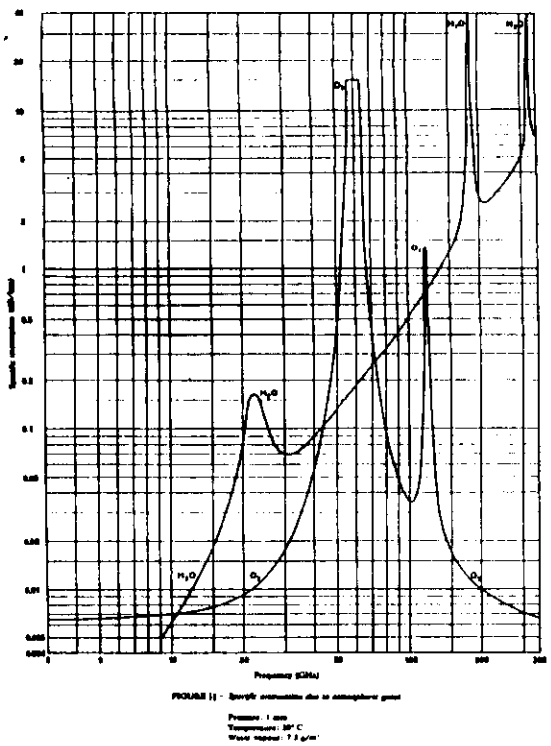

Fig.12 SPECIFIC ATTENUATION DUE TO OXYGEN AND WATER VAPOUR

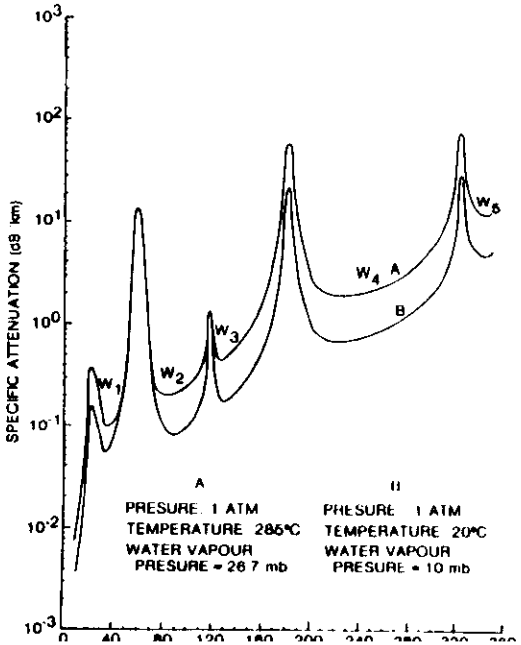

where h_{wo} = water vapour equivalent height in the window regions.

= 1.6 km in clear weather

= 2.1 km in rain.

The scale heights, hence the equivalent heights for oxygen and water vapour may vary with latitude, season and/or climate. The water vapour height profile in the real atmosphere may differ considerably from the exponential with consequent changes in equivalent heights.

for elevation angle, θ greater than 10°

$$A_a = \frac{h_o \gamma_o + h_w \gamma_w}{\sin\theta} \quad - - - \quad (40)$$

Equation (38) assumes temperature of 15°C on ground. For other temperatures, h_w is increased by 0.1% or 1% per deg. C in clear weather or rain resp., in the window regions and by 0.2% or 2% per deg. C in the absorption bands (CCIR, 1986)

7.1.2 Alternative Approach

At the surface of the earth (p = 1000 mb),

$$\gamma_a = a + bp - ct \quad - - - - \quad (41)$$

where

p = surface water vapour concentration g/m³

t = surface air temperature, °C.

a, b, c are empirical coefficients derived by multiple regression analysis, which vary with operating frequency, f. Table 6 (CCIR, 1982)

Frequency f(GHz)	Coefficients		
	a(f)	b(f)	c(f)
1	0.00588	0.0000178	0.000517
4	0.00802	0.000141	0.0000850
6	0.00824	0.000300	0.0000895
12	0.00898	0.00137	0.000108
15	0.00953	0.00269	0.000125
16	0.00976	0.00345	0.000133
20	0.0125	0.0125	0.000101
22	0.0181	0.0221	0.000129
24	0.0162	0.0203	0.0000563
30	0.0179	0.0100	0.000280
35	0.0264	0.0101	0.000369
41	0.0499	0.0121	0.000620
45	0.0892	0.0140	0.00102
50	0.267	0.0171	0.00251
55	3.93	0.0220	0.0158
70	0.449	0.0319	0.00443
80	0.160	0.0391	0.00130
90	0.113	0.0495	0.000744
94	0.106	0.0540	0.000641
110	0.116	0.0749	0.000644
115	0.206	0.0826	0.00185
120	0.985	0.0931	0.0115
140	0.123	0.129	0.000372
160	0.153	0.206	0.000784
180	1.13	1.79	−0.00237
200	0.226	0.366	0.00167
220	0.227	0.316	0.000174
240	0.258	0.356	−0.000119
280	0.336	0.497	−0.0000664
300	0.379	0.629	0.000808
310	0.397	0.812	0.00286
320	0.732	2.36	0.00467
330	0.488	1.61	0.00945
340	0.475	1.06	0.00519
350	0.528	1.23	0.00722

Table 6: Coeffients for computing specific attenuation at the surface due to gaseous contributions. [CCIR, 1982]

Frequency f(GHz)	Coefficients		
	α(f)	β(f)	ξ(f)
1	0.0334	0.00000276	0.000112
4	0.0397	0.000276	0.000176
6	0.0404	0.000651	0.000196
12	0.0436	0.00318	0.000315
15	0.0461	0.00634	0.000455
16	0.0472	0.00821	0.000536
20	0.0560	0.0346	0.00155
22	0.0760	0.0783	0.00310
24	0.0691	0.0591	0.00250
30	0.0850	0.0237	0.00133
35	0.123	0.0237	0.00149
41	0.237	0.0284	0.00211
45	0.426	0.0328	0.00299
50	1.27	0.0392	0.00572
55	24.5	0.0490	−0.00121
70	2.14	0.0732	0.0104
80	0.705	0.0959	0.00586
90	0.458	0.122	0.00574
94	0.417	0.133	0.00594
110	0.431	0.185	0.00785
115	0.893	0.203	0.0113
120	5.35	0.221	0.0363
140	0.368	0.319	0.0119
160	0.414	0.506	0.0191
180	2.81	5.04	0.192
200	0.562	0.897	0.0339
220	0.543	0.777	0.0276
240	0.601	0.879	0.0307
280	0.760	1.22	0.0428
300	0.853	1.54	0.0551
310	0.905	1.97	0.0735
320	1.66	6.13	0.238
330	1.13	3.94	0.155
340	1.07	2.56	0.0969
350	1.20	2.96	0.114

Table 7: Coefficients for computing total zenith attenuation. [CCIR, 1982].

shows the values of a, b, c

The total zenith attenuation τ_{90} based on the global data set is given by

$$\tau_{90} = \alpha + \beta\rho - \xi t \quad ---(42a)$$

where $\rho = 216.7 \cdot \frac{e}{T}$ ---(42b)

ρ = water vapour concentration at the surface, g/m^3, e is water vapour pressure in mb, T = surface air temperature in K, t = surface air temperature in °C.

α, β, ξ are empirical coeffs. from multiple regression, which are frequency dependent (Table 7, CCIR, 1982)

for inclined paths the atmospheric attenuation may be assumed proportional to the effective distance through the attenuation medium as approximated by

$$\therefore \tau(\theta) = \tau_{90} \cdot \frac{r_a}{H_a} = \gamma_a r_a \quad ---(43)$$

where

r_a = effective slant path

$$r_a = \frac{2H_a}{\sqrt{\sin^2\theta + 2\frac{H_a}{R}} + \sin\theta} \quad \text{for } \theta \leq 10^\circ \quad ----(44)$$

for $\theta > 10^\circ$

$$r_a = \frac{H_a}{\sin\theta} \quad ----(45)$$

where H_a = combined scale height of water vapour and oxygen.

$$H_a = \tau_{90} / \gamma_a \quad ----(46)$$

The attenuation on a slant path at an elevation angle θ from the surface to a height h is given by

$$A = \gamma r_a [1 - \exp(-h/H_a)] \quad ---(47)$$

8 REFERENCES

1. Ajayi, G.O.: "Rain induced attenuation and phase shift at cm and mm waves using a tropical raindrop size distribution model." Int. Sym. Antennas and Propagation, ISAP, Kyoto, Japan, 1095-1098, 1985.

2 Ajayi, G.O.: "Characteristics of rain induced attenuation and phase shift at cm and mm waves using a tropical raindrop size distribution model, Int. J. Infrared and mm. waves, 6, 8, 771-806, 1985.

3 Ajayi, G.O. and Olsen, R.L.: "Measurements and analysis of raindrop size distribution in South West Nigeria, URSI Commission F Symp. on Wave Propagation and Remote Sensing, Louvain-La-Neuve, Belgium, 173-184, 1983.

4 Ajayi, G.O. and Ofoche, E.B.C.: "Some tropical rainfall rate characteristics at Ile-Ife for microwave and millimetre wave applications" Journ. of Climate and Applied Meteorology, 23, 562-567, 1984.

5 Ajayi, G.O. and Olsen, R.L.: "Modeling of a tropical rain dropsize distribution for microwave and millimetre wave applications, Radio Science, 20, 193-202, 1985.

6 Ajayi, G.O., Owolabi, I.E. and Adimula, I.A.; "Rain induced depolarization from 1GHz to 300 GHz in a tropical environment, Int. J. of Infrared and mm. waves, 8, 177-197, 1987

7 CCIR: Recommendations and Reports of the International Radio Consultative Committee, XVth Plenary Assembly – Propagation in non-ionized media, Vol. V, 1982.

8 - - - - -, Vol. V, 1986.

9 CCIR: Conclusions of the Interim Meeting of Study Group 5 – Propagation in non-ionized media, Doc. 5/204-E, July 1988.

10 Gibbins, C.J.: "Improved algorithms for the determination of specific attenuation at sea by dry air and water vapour in the frequency range 1-300 GHz", Radio Science, 21, 945-954, 1986.

11. Ippolito, L.J.: Radio propagation for space communications Systems, Proc. IEEE, 69, 1981

12 Ippolito, L.J., Kaul, R.D. and Wallace, R.G.: Propagation Effects Handbook for Satellite Systems Design. A Summary of Propagation Impairments on 10 to 100 GHz Satellite Links With Techniques for System Design" NASA, U.S.A. Reference Publication 1082 (03), 1983

13 Joss, J., Thams, J.C. and Waldvogel, A.: "The variation of raindrop size distributions at Locarno. Proc. Int. Conf. Cloud Physics, Toronto, Canada, 369-373, 1968.

14 Laws, J.O. and Parson, D.A.: "The relation of raindrops with size, J. of Meteor., U.S.A, 5, 165-166, 1948.

15 Maggiori, D.: "Computed transmission through rain in the 1-400 GHz frequency range for spherical and elliptical drops and any polarization", Fub Report IC379, Alta frequenza, 5, 262-273, 1981.

16. Marshall, J.S and Palmer, W.M.: "The distribution of raindrops with size", J. of Meteor., U.S.A., 5, 165-166, 1948

17. Manpfourma, f.: "Model of rainfall rate distribution for radio system design," IEE Proc. 132, Pt. H, 1, 39-43, Feb. 1985(b).

18 Manpfourma, F.: "Atlas mondial des intensites de pluie an 1 minute", Note tech. CMET. (MER/RPE), France, Dec. 1985(b).

19 Manpfourma, F.: "More about rainfall rates and their prediction for radio systems engineering", Proc. IEE, Part H, 134, 6, 527-537, 1987.

20 Oguchi, T.: "Electromagnetic wave propagation and scattering in rain and other hydrometeors", Proc. IEEE, 71, 1029-1078, 1983

21 Olsen, R.L, Rogers, D.V. and Hodge, D.B.: "The aR^b relation in the calculation of rain attenuation" IEEE Trans. Ant. and Propagation, AP-26, 318-329, 1978

22 Pruppacher, H.R. and Pitter, R.L.: "A semi-empirical determination of the shape of cloud and raindrops. J. Atmos. Sci., 28, 86-94, 1971.

23 Reddy, B.M.: "Physics of the Troposphere, in Handbook on Radiopropagation for tropical and sub-tropical countries, 59-77, 1987.